Elastic backscattering measurements for ^{6}Li+^{28}Si at sub- and near-barrier energies

K. Zerva,[1] N. Patronis,[1] A. Pakou*,[1] N. Alamanos,[2] X. Aslanoglou,[1] D. Filipescu,[3] T. Glodariu,[4] M. Kokkoris,[5] M. La Commara,[6] A. Lagoyannis,[7] M. Mazzocco,[8] N. G. Nicolis,[1] D. Pierroutsakou,[9] M. Romoli,[9] and K. Rusek[10]

[1] *Department of Physics, The University of Ioannina, 45110 Ioannina, GREECE*

[2] *DSM/DAPNIA CEA SACLAY, 91191 Gif-sur-Yvette, FRANCE*

[3] *"Horia Hulubei" National Institute of Physics and Nuclear Engineering, 077125 Magurele, ROMANIA*

[4] *"Horia Hulubei" National Institute of Physics and Nuclear Engineering, ROMANIA*

[5] *National Technical University of Athens-GREECE*

[6] *Dipartimento di Scienze Fisiche and INFN Sezione di Napoli, I-80125, Napoli, ITALY*

[7] *National Research Center Demokritos-GREECE*

[8] *Dipartimento di Fisica, INFN, I35131 Padova, Italy*

[9] *INFN Sezione di Napoli, I-80125, Napoli, ITALY*

[10] *Heavy Ion Laboratory, University of Warsaw , Pasteura 5a, 02-093 Warsaw, POLAND*

(Dated: May 27, 2009)

Abstract

Elastic backscattering measurements were performed for the weakly bound nucleus ^{6}Li on a ^{28}Si target at sub- and near-barrier energies (0.6 to 1.3 $V_{C.B.}$). Excitation functions of elastic scattering cross sections were measured at 150^{0} and 170^{0} and the corresponding ratios to Rutherford scattering and relevant barrier distributions were formed. The results are discussed in terms of the potential threshold anomaly and the reaction mechanisms involved.

PACS numbers: 25.70.Bc, 24.10.Ht, 24.50.+g

* corresponding author, e-mail: apakou@cc.uoi.gr

As it is well known for heavy ion reactions, approaching the vicinity of the Coulomb barrier, couplings between various channels increase in importance. Describing elastic scattering, either these couplings have to be taken into account through coupled channel theories, or the energy dependence of the various optical model parameters has to be considered explicitly. In fact, the term "threshold anomaly" was invoked to describe a rapid variation of such model parameters around the barrier in well bound nuclei. In that respect, near- and sub-barrier fusion cross sections have been reproduced [1, 2] by using a single barrier penetration model with an energy dependent potential corresponding to the threshold anomaly. Moving to weakly bound nuclei the situation becomes more complicated due to the influence of breakup and/or transfer effects. In fact for ^{6}Li, in contrast to the well bound nuclei, an absence of the threshold anomaly was reported previously [3, 4], while later [5, 6], an increasing trend approaching the barrier was determined for the imaginary part of the polarization potential. This was related to a rather flat or slightly curved with negative slope trend for its real part, in accordance with dispersive relations. The proposed new type of anomaly was based on a systematic data analysis of ^{6}Li elastic scattering on various targets (^{28}Si, ^{58}Ni, ^{118}Sn, ^{208}Pb), measured previously [5, 7, 8], in the context of double folding model [9] by using the BDM3Y1 interaction developed by Khoa et al. [10]. This trend, verified in [11, 12] by using the Sao Paulo potential [13], was attributed to breakup and therefore named as breakup anomaly. In principle, the lack of sensitivity for obtaining the energy dependence of potential parameters, at energies close to the coulomb barrier, leads occasionally to vague conclusions, while the determination of such dependence at sub-barrier energies is almost impossible. In order to improve our understanding on the energy dependence of the potential especially at sub-barrier energies and the relevant processes involved in the threshold anomaly, other complementary means should be adopted. In this respect, we test in this work excitation functions of backscattering measurements as a tool for probing the new type potential anomaly for weakly bound nuclei, at near as well as at sub-barrier energies. The knowledge of the optical potential at deep sub-barrier energies in an accurate way is especially useful for nuclear astrophysics and nucleosynthesis studies.

The last years a large amount of work has been devoted on systematic studies of the nuclear potential surface properties through high precision back-angle quasi-elastic scattering measurements [14–19] at sub-barrier energies. At these backward angle studies, deviations from unity of the elastic to Rutherford cross section ratios, are sensitive mainly to the surface

properties of the potential [15].

Moreover, barrier distributions of elastic [20] and quasi-elastic scattering [21], obtained via first derivatives as follows

$$D_{el}(E) = -\frac{d}{dE}\left[\sqrt{\frac{d\sigma_{el}}{d\sigma_{Ruth}}(E)}\right],\ D_{qel}(E) = -\frac{d}{dE}\left[\frac{d\sigma_{qel}}{d\sigma_{Ruth}}(E)\right] \quad (1)$$

have been used mainly on research with stable projectiles to probe channel coupling effects at barrier energies [21–27], in almost the same effective way as barrier distribution from fusion measurements, initially presented in ref. [28].

The influence of direct processes on elastic scattering and other reaction channels with weakly bound nuclei has been reviewed in [29, 30]. A first measurement with a weakly bound projectile has been performed recently on ^{6}Li+^{144}Sm and reports backward elastic and quasi-elastic barrier distributions [31] with emphasis on breakup coupling to elastic scattering. For the system ^{6}Li+^{28}Si, strong transfer channels were reported in [32–34] while a weak breakup channel was reported in [35] . Then, the arising question is : Does transfer or breakup influence elastic scattering and the other reaction processes at barrier energies?

In the following, we report a back-angle elastic scattering excitation function measurement for ^{6}Li+^{28}Si at sub- and near-barrier energies aiming to further enlight the subjects stated above, concerning the new type of potential anomaly and relevant reaction mechanisms. Experimental data were analyzed with an energy dependent optical potential liable to the threshold anomaly, taking care for a reproduction of previously measured total reaction and fusion cross sections [34]. The results were considered also in the context of a coupled channel description, where breakup is explicitly taken into account.

^{6}Li^{3+} beams were delivered by the TN11/25 HVEC 5.5 MV Tandem accelerator of the National Research Center of Greece-DEMOKRITOS at several bombarding energies, from 5 to 11 MeV. Beam currents were of the order of 5 nA. The beam impinged on a 200 μg/cm^2 thick, self supporting ^{28}Si target, at a target frame fixed perpedicular to the beam direction. Backscattering elastic events were recorded in four silicon detectors set at $\pm$150 and $\pm$ 170 degrees. The beam flux was recorded via the Rutherford scattering in two silicon detectors set at $\pm$ 30 degrees. Subsequently elastic cross section ratios to Rutherford were formed as follows

$$\frac{\sigma_{el}}{\sigma_{Ruth}}(170^0 - 150^0) = \frac{N(170^0 - 150^0)}{N(30^0)}\frac{\sigma_{Ruth}(30)}{\sigma_{Ruth}(170)}\frac{\Omega_{30}}{\Omega_{170(150)}} \quad (2)$$

where N_{30} and $N_{170(150)}$ is the elastic scattering counting rate at forward and backward detectors, and Ω_{30}, $\Omega_{170(150)}$ are the solid angles subtended by the forward and backward detectors The ratio of solid angles was determined in the same experiment by using a thin gold target and by using lithium ions at 11 MeV. At this energy, the elastic scattering is pure Rutherford for both forward and backward detectors, and the ratio of solid angles can be determined with a negligible error. Therefore the only error involved in relation (2) is the statistical error which in most of the energies was less than 2%, except at the highest energies which was up to 20%. The obtained excitation functions are presented in Figure 1a and the corresponding barrier distributions, determined by using a point difference formula for extracting the derivative of relation (2)-first expression, are presented in Figure 1b. A first inspection of this figure shows the absence of the usual second peak at energies above the nominal coulomb barrier related to inelastic excitations. This was expected however, since preliminary coupled channel calculations with the code ECIS showed that inelastic excitations of both target and projectile are negligible and such couplings can be omitted. Also in our particle spectra inelastic excitation peaks were not present to an extend of cross section production less than 2 mb at the highest energy.

Having obtained excitation functions and barrier distributions, we proceed with our theoretical analysis. It should be noted that the results presented in Figure 1 are mean cross sections of the ones obtained at 150 and 170 degrees, since the energy centrifugal correction was negligible ($\sim$ 1.8%). In Figure 2 we present previous data on the potential anomaly, obtained in a folding framework [5] with a BDM3Y1 interaction . While the increasing trend is obvious for the heavier targets, for ^{28}Si due to the large assigned errors this is not clear. In this analysis, in order to describe the imaginary part of the potential, we choose three different lines with increasing slopes and a line with decreasing slope as we approach the barrier and we calculate through dispersive relations [6, 36] the real potential. With this optical potential, elastic scattering cross sections are calculated for backward angles (150 and 170^0). The results, a mean of cross sections at 150 and 170^0, are presented in Figure 1a. The corresponding barrier distributions are presented in Figure 1b. It is obvious especially from the comparison with the barrier distribution data that a decreasing behaviour for the imaginary potential is totally excluded for the system ^{6}Li+^{28}Si. For the increasing behaviour of the imaginary potential we note the following. The steepest slope corresponds to a flat barrier distribution shifted to the left off the barrier distribution obtained with a

"bare" potential (normalization factors to the BDM3Y1 interaction equal to one). As the slope is reduced the barrier distribution is shifted to the right and the height of the barrier distribution maximum increases. We note that for our system the best of the three lines representing the imaginary part of the potential is the one with the smaller slope (blue solid line-Figure 2). The connection between the slope of the line describing the imaginary potential and the involved direct process (breakup or/and transfer) is not straight forward and needs further investigation. In that direction complementary measurements with lighter and heavier targets are under the way. Last, in order to fully map the energy dependence of our potential we have however to fix the point after which the potential drops to zero. From Figure 2 we see that, if we choose an "early" drop of the potential the barrier distribution while keeps the height of its maximum has been moved to the left. It has become clear with the above analysis that barrier distributions of elastic scattering can be proved a valuable tool for tracing the threshold anomaly and therefore the optical potential at near and sub-barrier energies.

To complete our analysis, we present in Figure 3 previously measured [35] excitation functions of total reaction (green circles) and fusion cross sections (black stars). The experimental results are compared with calculations obtained with the above obtained "best" potential (black lines) and the code ECIS. The reproduction of the data is adequately good.

Subsequently we proceed with calculations in a coupled channel approach taking into account breakup. Our calculations followed closely those presented in [6]. Two body, $\alpha + d$ cluster model of ^{6}Li was assumed. The continuum above the $^6\mathrm{Li} \rightarrow \alpha + d$ breakup threshold was truncated at momentum $k = 0.52$ fm^{-1} and discretized into momentum bins of the 0.26 fm^{-1} width. Couplings between resonant and non-resonant cluster states corresponding to $\alpha - d$ relative orbital angular momentum $L = 0, 1, 2$ were taken into account by means of continuum - discretized coupled - channel method. Two resonances, at 2.18 MeV and 4.31 MeV of excitation energy, were also included. The diagonal and coupling potentials were calculated from empirical $\alpha + {}^{28}$Si and $d + {}^{28}$Si optical model potentials by means of single - folding technique. The results of the calculations are presented in Figure 4 with the solid curves: Figure 4a for the elastic scattering and Figure 4b for the barrier distribution, and show very good agreement with the data. The dotted-dashed curves represent results of optical model calculations, without couplings to the breakup states from the continuum included. In Figure 3, the results of calculations for the total reaction cross section and the

fusion cross section are plotted and show fair agreement with the data.

In conclusion, we have shown that by determining experimentally barrier distributions via elastic scattering at backward angles we have an additional tool to map the optical potential at near and sub- barrier energies, where weakly bound nuclei present the new type of threshold anomaly. The proposed method, is especially useful for sub- and deep sub-barrier energies, where the nuclear field is weak and manifested only at very backward-angle data. Our coupled channel analysis shows that breakup, although a weak channel for the studied system, is a strong channel coupling element at barrier energies. On the other hand, the influence of transfer, which is a strong direct channel at sub- and near barrier energies, has to be also investigated.

---

[1] G.R. Satchler, Phys. Reports **199**, 147 (1991).

[2] M. A. Nagarajan and G.R. Satchler, Phys. Lett. **B 173**, 29 (1986).

[3] N. Keeley et al., Nucl. Phys. A571, 326 (1994).

[4] A. M. M. Maciel et al., Phys. Rev. C 59, 2103 (1999).

[5] A. Pakou et al., Phys. Lett. **B 556**, 21 (2003).

[6] A. Pakou et al., Phys. Rev. **C 69**, 054602 (2004).

[7] N. Keeley et al., Nucl. Phys. **A 571**, 326 (1994).

[8] K. O. Pfeifer, E. SPeth, K. Bethge, Nucl. Phys. **A 206**, 545 (1973).

[9] G.R. Satchler and W.G. Love, Phys. Rep. **55** (1979) 183.

[10] D.T. Khoa et al., Phys. Lett. B 342 (1995) 6.

[11] M.S.Hussein, P. R. S. Gomes, J. Lubian, L. C. Chamon, Phys. Rev. **C 76**, 019901(E) (2007).

[12] J. M. Figueira et al., Phys. Rev. **C 75**, 017602 (2007).

[13] M. A. Candido Ribeiro, L.C. Chamon, D. Pereira, M.S. Hussein, D. Galetti, Phys. Rev. Lett **78**, 3270 91997).

[14] I.I. Gontchar, D. J. Hinde, M. Dasgupta, J. O. Newton, Nucl. Phys. **A 722**,479c(2003).

[15] K. Hagino, T. Takehi, A. B. Balantekin, and N. Takigawa, Phys. Rev. **C 71**, 044612 (2005).

[16] K. Washiyama, K. Hagino, M. Dasgupta, Phys. Rev. **C 73**, 034607 (2006).

[17] L. R. Gasques et al., Phys. Rev **C 76**, 024612 (2007).

[18] O. A. Capurro, Niello J. O. Fernandez , A. J. Pacheco, P. R. S. Gomes, Phys. Rev. **C 75**,

047601 (2007)

[19] M. Evers et al., Phys. Rev. **C 78**, 034614 (2008)

[20] N. Rowley, G. R. Satchler, and P. H. Stelson, Phys. Lett. **B 524**, 25 (1991).

[21] H. Timmers et al., Nucl. Phys. **A 584**, 190 (1995).

[22] N. Rowley et al., Phys. Lett. **B 373**, 23 (1996).

[23] H. Timmers et al.,J. Phys. **G 23**, 1175 (1997).

[24] H. Timmers et al., Nucl. Phys. **A 633**, 421 (1998).

[25] R. F. Simoes et al., Phys. Lett. **B 527**, 187 (2002).

[26] E. Piasecki et al.,Phys. Rev **C 65**, 054611(2002).

[27] J. M. B. Shorto et al., Phys. Rev. **C 78**, 064610 (2008).

[28] N. Rowley, G. R. Satchler and P. H. Stelson, Phys. Lett. **B 524**, 25(1991).

[29] L. F. Canto, P. R. S.Gomes, R. Donangelo, M. S. Hussein, Phys. Rep. **424**, 1(2006).

[30] N. Keeley, R. Raabe, N. Alamanos, J. L. Sida, Prog. Part. and Nucl. Phys. **59**, 579(2007).

[31] D. S. Monteiro et al., Phys. Rev **C 79**, 014601(2009).

[32] A. Pakou et al., Phys. Rev. **C 76**, 054601(2007).

[33] A. Pakou, Phys. Rev. **C 78**, 067601 (2008).

[34] A. Pakou et al., Eur. Phys. J. **A 39**, 187(2009).

[35] A. Pakou et al., Phys. Lett. **B 633**, 691(2006).

[36] C. Maxaux, H. Ngo, G. R. Satchler, Nucl. Phys. **A 449**, 354 (1986).

[37] Ricardo A. Broglia and Aage Winther, Heavy Ion Reactions, Volume I: Elastic and Inelastic Reactions; The Benjamin/ Cummings Publishing Company, Inc (1981).

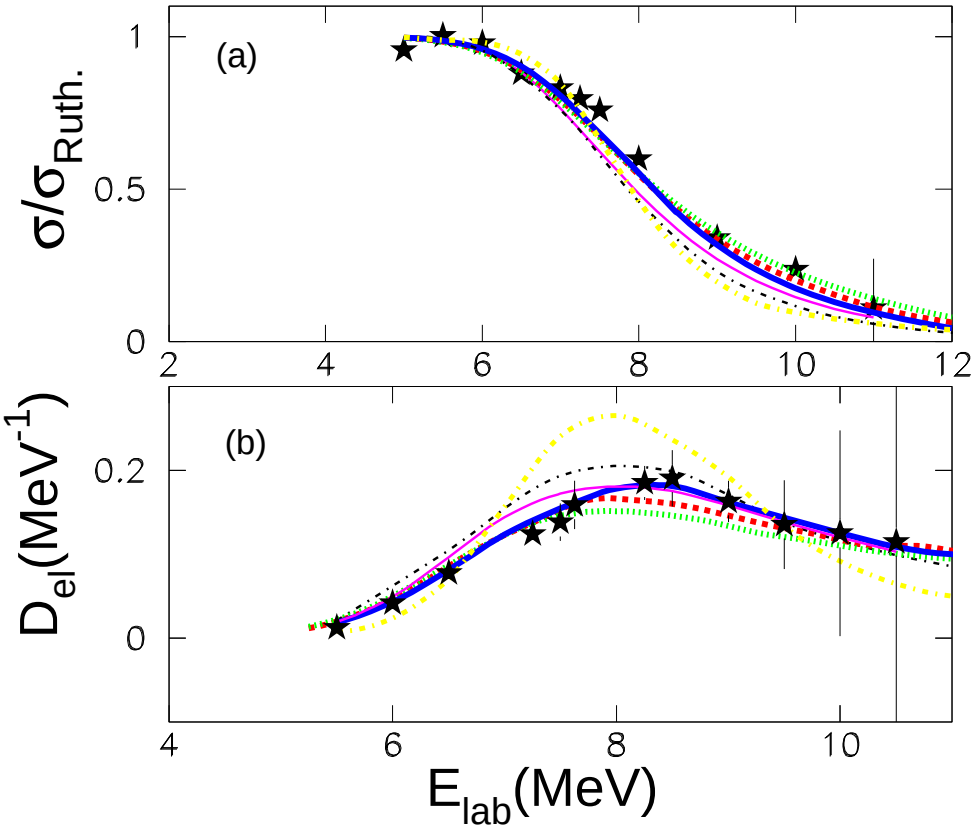

FIG. 1: (a) Elastic cross sections (designated by stars), measured at 150 and 170^0 (mean cross section) as a function of energy for ^{6}Li+^{28}Si. The lines represent ECIS calculations with the optical potential presented in Figure 2, with the same notation. The yellow dotted-dashed line corresponds to a decreasing imaginary potential, the green dotted line with an increasing imaginary potential with the steepest slope, the red dashed line with an increasing potential but with smaller slope, the blue solid line with increasing imaginary potential but with the smallest slope, the pink thin solid line with the last imaginary potential but which drops to zero earlier, and last the black dotted-dashed line to a "bare" potential where the normalization factor of the interaction for both real and imaginary parts of the potential was set equal to one. (b) Elastic backscattering barrier distributions, with the same notation as in (a)

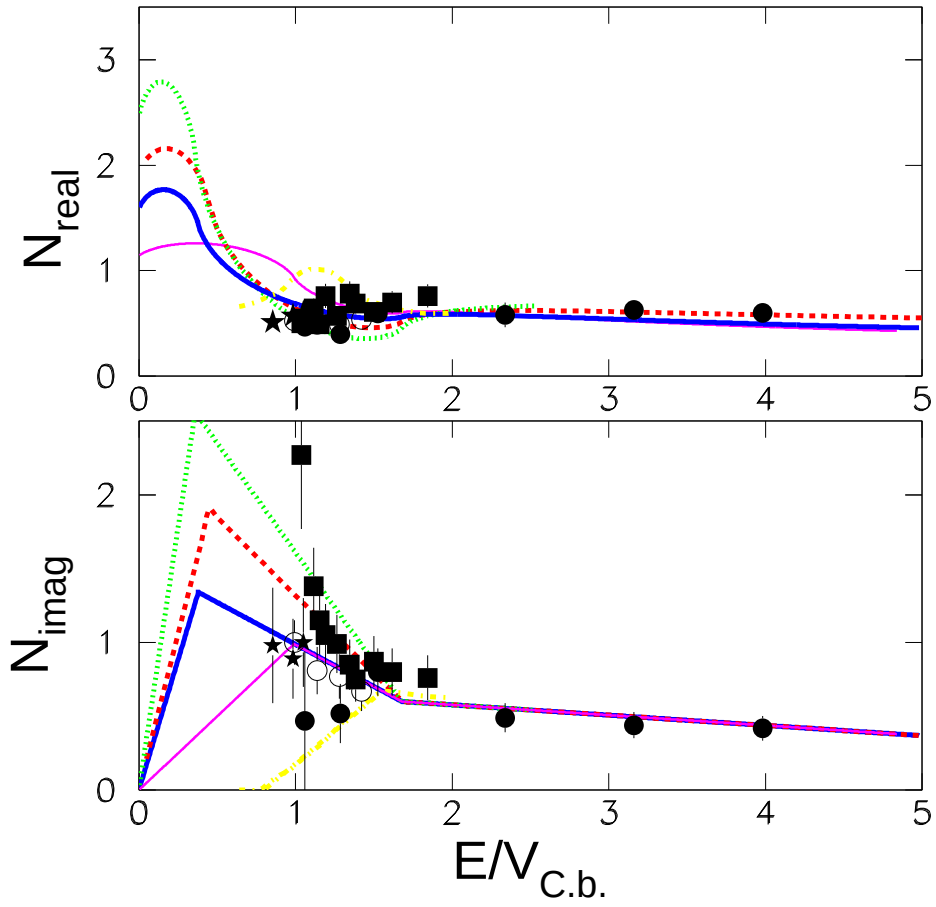

FIG. 2: Previously determined normalization factors of the real and imaginary potential as a function of the ratio of lithium bombarding energy over the barrier [5, 6]. Solid circles correspond to data for the ^{6}Li+^{28}Si system, open circles to the ^{6}Li+^{118}Sn, stars to the ^{6}Li+^{58}Ni system and cubes to the ^{6}Li+^{208}Pb system. The adopted barriers in the laboratory, equal to 8.54, 14.1, 26.6 and 31.22 MeV for the above systems respectively according to relations included in [37]. For the imaginary potential we have assumed five different descriptions related with the existing data (dotted-dashed yellow, dotted green, dashed red, solid blue and thin solid pink lines). The corresponding real potential was calculated via dispersive relations.

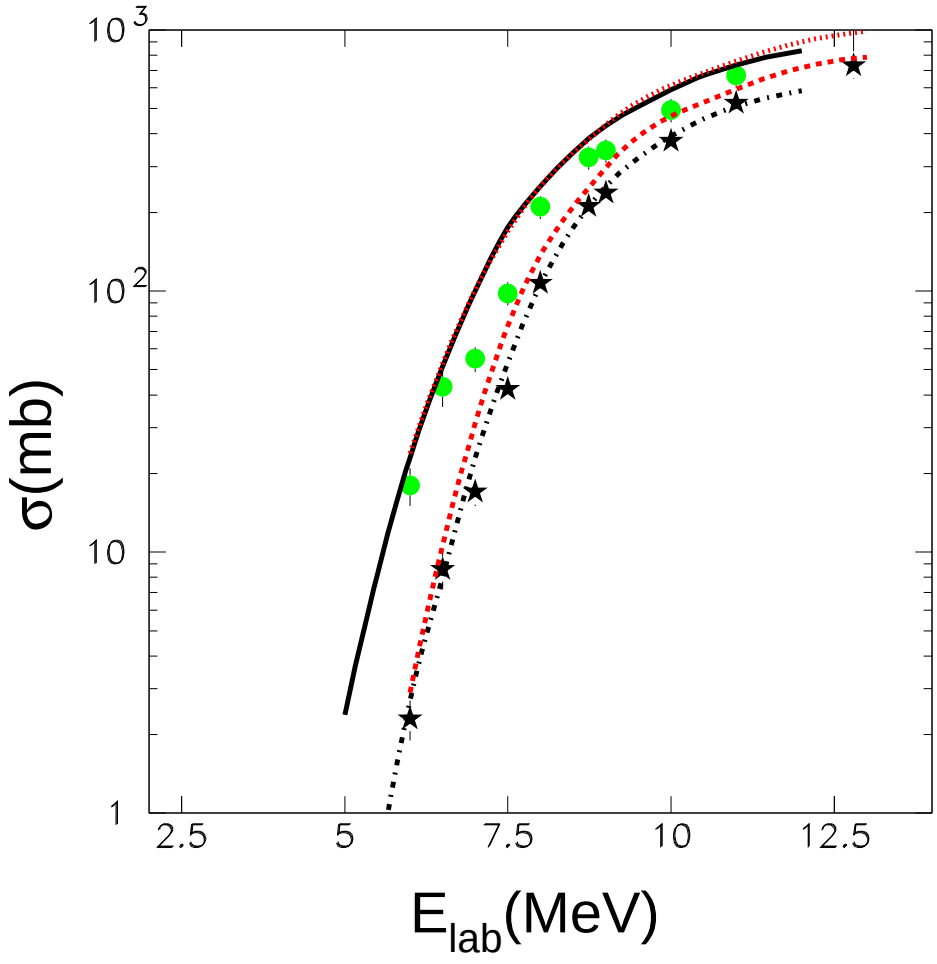

FIG. 3: Total reaction (green circles) and fusion cross section (black stars) measurements as a function of energy reported previously[33]. The black solid and dotted-dashed lines are ECIS calculations for total reaction and fusion cross sections respectively, corresponding to the "best" optical potential (Figure 2, blue line). The red dotted and dashed lines show coupled channel calculations for the total reaction and fusion cross sections, respectively.

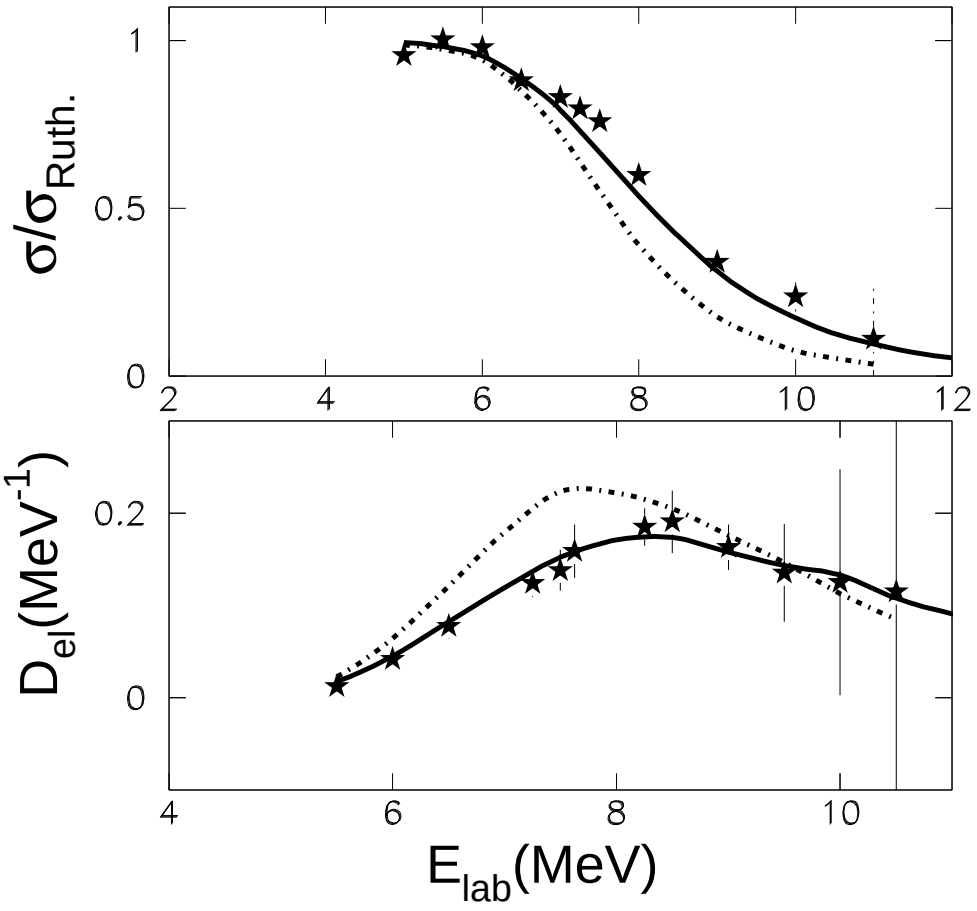

FIG. 4: The elastic scattering data and corresponding barrier distributions, presented in Figure 1, are compared with coupled channel calculations (dotted dashed line-bare potential calculations, solid line-coupled channel calculations)